Conf-9304131--7

2

DEVELOPMENT AND APPLICATION OF THE AUTOMATED MONTE CARLO BIASING PROCEDURE IN SAS4

J. S. Tang and B. L. Broadhead
Computing Applications Division
Oak Ridge National Laboratory*
P.O. Box 2008
Oak Ridge, Tennessee USA 37831-6370

To be presented at the
Seminar on Advanced Monte Carlo Computer
Programs for Radiation Transport
April 27-29, 1993
Centre d'Etudes, Saclay, France

*Managed by Martin Marietta Energy Systems, Inc., under contract DE-AC05-84OR21400 with the U.S. Department of Energy.

DEVELOPMENT AND APPLICATION OF THE AUTOMATED MONTE CARLO BIASING PROCEDURE IN SAS4

J. S. Tang and B. L. Broadhead
Computing Applications Division
Oak Ridge National Laboratory
P.O. Box 2008
Oak Ridge, Tennessee USA 37831-6370

ABSTRACT

An automated approach for biasing Monte Carlo shielding calculations is described. In particular, adjoint fluxes from a one-dimensional discrete-ordinates calculation are used to generate biasing parameters for a three-dimensional Monte Carlo calculation. The automated procedure consisting of cross-section processing, adjoint flux determination, biasing parameter generation, and the initiation of a MORSE-SGC/S Monte Carlo calculation has been implemented in the SAS4 module of the SCALE computer code system.

The automated procedure has been used extensively in the investigation of both computational and experimental benchmarks for the NEACRP working group on shielding assessment of transportation packages. The results of these studies indicate that with the automated biasing procedure, Monte Carlo shielding calculations of spent fuel casks can be easily performed with minimum effort and that accurate results can be obtained at reasonable computing cost. The systematic biasing approach described in this paper can also be applied to other similar shielding problems.

I. INTRODUCTION

SAS4[1] is a module in the SCALE computer code system[2] which was developed by the Computing Applications Division of Oak Ridge National Laboratory. The primary task of SAS4 is to perform a three-dimensional (3-D) Monte Carlo shielding analysis of a spent fuel cask using an automated biasing procedure. The automated procedure consists of cross-section processing, adjoint flux calculation, biasing parameter generation, and the initiation of a Monte Carlo calculation.

In Monte Carlo shielding analysis of a deep-penetration problem such as a spent fuel cask, variance reduction techniques must be employed in order to calculate reasonably good results at an affordable cost. Theoretically,[3,4] a single Monte Carlo history is sufficient to solve any problem if the adjoint flux is used to bias the selection of particle parameters (i.e., position, energy, and direction). However, from a practical standpoint, calculation of the adjoint flux and subsequent selection from the biased distributions would have required a greater computational expense than an unbiased solution to the original problem. Therefore, to achieve a reduction in the cost of the calculation, this optimal biasing procedure must be approximated.

In this work, the adjoint flux for the actual shipping cask is approximated by that obtained for a geometrically simplified [one-dimensional (1-D)] cask model. The adjoint flux for the simplified model is obtained from a discrete-ordinates calculation with the XSDRNPM-S code in the SCALE system.[2] Another practical problem associated with the use of the adjoint flux to bias Monte Carlo histories is that sampling from the adjoint-biased distribution must be carried out efficiently. This difficulty has been overcome by using the biasing schemes available in the MORSE-SGC/S code in the SCALE system, and the XSDRNPM-S adjoint fluxes are used to specify the biasing parameters needed to implement these techniques. The entire procedure for adjoint flux calculation, generation of Monte Carlo biasing parameters, and Monte Carlo calculation of radiation doses exterior to a spent fuel cask has been developed and described in this paper.

The automated biasing procedure is presented in the next section, followed by the description of the biasing techniques and generation of the biasing parameters. Application of the automated procedure to two recent studies on shipping casks dose-rate evaluations is described. The two studies are (1) a series of calculations for computational benchmarks for the NEACRP working group on shielding assessment of transport packages[5] and (2) the analysis of a series of dose rate measurements for a transport cask loaded with unconsolidated PWR spent fuel.[6] Finally, conclusions and discussion are given in the last section.

II. AUTOMATED BIASING PROCEDURE

The automated biasing procedure in SAS4 basically consisted of five steps:

1. processing of multigroup cross-section data which includes resonance self-shielding and optionally cell-weighting treatments;

2. calculation of adjoint fluxes of a simplified 1-D slab model of a cask using the XSDRNPM-S program;

3. processing of the adjoint fluxes into different biasing parameters;

4. application of the biasing parameters to the particle random walk in a Monte Carlo calculation with the MORSE-SGC/S code; and

5. estimation of radiation doses exterior to the cask.

This paper focuses on the discussion of the last four steps because they pertain to Monte Carlo study. For Monte Carlo shielding analysis of a spent fuel cask, the purpose of biasing (or importance sampling) is to encourage and increase the propagation of radiation particles toward the outside of the cask so that better estimates of exterior dose rates can be obtained. Since nuclear fuel casks generally have a long cylindrical shape, it is difficult to effectively bias particles simultaneously toward all three sides of a cask. For this reason, the Monte Carlo cask geometry used in this work is assumed to be symmetrical about the midplane perpendicular to the axial dimension. Even with the axially symmetric cask model, the radial and axial characteristics of particle transport may be drastically different due to the geometric shape, the shielding materials, and possibly the streaming effect in the fuel. Because of these complications, separate Monte Carlo calculations with different biasing procedures are required for radial and axial detectors. For radial detectors, the particle random walk is biased radially toward the side. For axial detectors, the particle random walk is biased axially away from the midplane and toward the top or bottom surfaces.

The adjoint discrete-ordinates calculation, from which biasing parameters are generated, is a 1-D slab model of either the radial or axial geometry of the cask being analyzed. The slab geometry starts with a spent fuel material that has a specular reflective boundary on one side and layers of materials simulating the radial or axial geometry of the cask on the other. Each material layer is identified as a zone in XSDRNPM-S. The thickness of the first zone is the height of spent fuel measured from the midplane for the axial geometry or the radius of the spent fuel for the radial geometry. If the spent fuel geometry in the Monte Carlo calculation is not cylindrical, a nominal radius is used as the thickness of the first zone in XSDRNPM-S. An adjoint source with a response function as the source spectrum located on the outermost surface of the slab geometry starts the adjoint calculation. The response function is either a neutron or gamma-ray fluence-to-dose conversion factor.

In MORSE-SGC/S, biasing takes place at each collision site and the biasing parameters are generally functions of energy group and spatial region (importance region). In the automated biasing procedure, a direct correspondence is made between the Monte Carlo importance regions and the zones in the adjoint discrete-ordinates calculation. Each zone in XSDRNPM-S corresponds to one or more importance regions in MORSE-SGC/S, depending on the optical thickness of the zone. The biasing parameters generated from adjoint fluxes are spatially averaged over the thickness of each importance region. During Monte Carlo random walk, biasings are implemented to each collision site according to the importance region in which the collision takes place. In this work, the importance region of a collision site is determined by the distance between the collision and the adjoint source surface. For radial responses, the adjoint source surface is the side surface; for axial responses, it is the top or bottom surface. Finally, the biasing parameters expressed as functions of energy group and/or spatial region are input or used directly in MORSE-SGC/S for calculation of external dose rates of the spent fuel cask.

III. BIASING TECHNIQUES AND GENERATION OF BIASING PARAMETERS

The MORSE-SGC/S biasing options used in this study are the source energy biasing, energy biasing at collision site, splitting and Russian roulette, and path-length stretching. The efficiency of a calculation is determined by the proper specification of these parameters. It has been shown[3,4] that a near-optimal importance function for selection of emergent particle parameters (i.e., energy and direction of a particle emerging from a source or a collision point) is the adjoint flux. The event-value function has been shown[7] to be the proper biasing function for path-length selection. In this work, these adjoint functions are generated for a 1-D cask model with XSDRNPM-S and are used to specify the biasing parameters for the biasing options in MORSE-SGC/S.

The theoretical development of Monte Carlo importance sampling in MORSE-SGC/S is given elsewhere[7,8] and will not be repeated here. Instead, each biasing technique and biasing parameter evaluation in the automated procedure is described in detail.

III.A ENERGY BIASING PARAMETERS AT COLLISION SITE, EPROB, AND SOURCE ENERGY BIASING PARAMETERS, BFS

For selection of the energy of a particle emergent from a collision site, $\phi^*(IG,IR)$ (the region-averaged and energy-dependent adjoint flux calculated by XSDRNPM-S) is used directly as the importance function EPROB(IG,IR) in MORSE-SGC/S; that is,

$$\text{EPROB}(IG,IR) = \phi^*(IG,IR),$$

where

IG = energy group number,
IR = region number.

Since a source particle can be regarded as a particle emergent from the zeroth collision site, source energy biasing is treated in the same manner; that is,

$$\text{BFS}(IG) = \phi^*(IG,1),$$

where

BFS = source energy importance function,
$\phi^*(IG,1)$ = adjoint flux in group IG averaged over region 1, which contains the spent fuel.

Then, the biased source energy distribution is

$$\hat{S}(IG) = \frac{S(IG)\phi^*(IG,1)}{\sum_{IG} S(IG)\phi^*(IG,1)}, \qquad (1)$$

where $S(IG)$ is the natural source spectrum.

SAS4 allows axial dependence of the source distribution in order to account for the spent fuel burnup profile. For calculations involving radial detectors (radial calculations), source particle axial locations are sampled directly from the specified distribution. However, for calculations involving axial detectors (axial calculations), the axial location of source particles is biased by the adjoint flux when the source distribution is axially uniform, but is sampled from an exponential function e^{CZ} when the source has an axial profile. The constant C is chosen such that $CZ_{max} = 5$, where Z_{max} is the source height measured from the midplane. The selection of the source location is independent of the selection of the source energy from Eq. (1).

III.B RUSSIAN ROULETTE AND SPLITTING PARAMETERS *WTAV, WTHI, WTLO*

Since it has been shown[9] that in near-optimal calculations particle statistical weights are inversely proportional to the adjoint flux, we set the weights of particles in regions *IR* with energy group *IG* as

$$\mathrm{WTAV}(IG,IR) = \frac{\lambda}{\phi^*(IG,IR)} , \tag{2}$$

where

WTAV = group- and region-dependent Russian roulette survival weight,
λ = effect of interest or the total response.

The total response is the sum of responses of each group that, in turn, can be computed from the product of the group source strength and the corresponding adjoint flux in the source region; i.e.,

$$\lambda = \sum_{IG} \lambda(IG) = \sum_{IG} S(IG)\phi^*(IG,1) .$$

Substituting Eq. (1) into the above, we have

$$\lambda = \frac{S(IG)\phi^*(IG,1)}{\hat{S}(IG)} .$$

Substitution of λ into Eq. (2) gives

$$\mathrm{WTAV}(IG,IR) = \frac{S(IG)\phi^*(IG,1)}{\hat{S}(IG)\phi^*(IG,IR)} . \tag{3}$$

In Eqs. (2) and (3), the quantities on the right side are known since the adjoint fluxes are calculated by XSDRNPM-S, and $\hat{S}(IG)$ is given by Eq. (1). Equation (2) or (3) is used to set the Russian roulette survival weight of each region and energy group throughout the entire system. Note from Eq. (3) that for the source region, WTAV is equal to $S(IG)/\hat{S}(IG)$, which is the statistical weight of source particles after source energy biasing. In a similar manner, the weight above which splitting occurs in zone *IR* and group *IG* is determined by the minimum adjoint flux in zone *IR* of group *IG*; i.e.,

$$\mathrm{WTHI}(IG,IR) = \frac{\lambda}{\phi^*_{\min}(IG,IR)} . \tag{4}$$

The weight below which Russian roulette is played is determined by the maximum ϕ^* in zone *IR* of group *IG*; i.e.,

$$\text{WTLO}(IG,IR) = \frac{\lambda}{\phi^*_{max}(IG,IR)} . \tag{5}$$

Finally, to regulate the values of WTHI and WTLO, limits had been set on ϕ^*_{max} and ϕ^*_{min} so that WTHI would be <100 * WTAV and WTLO would be >WTAV/100.

III.C PATH-LENGTH STRETCHING PARAMETERS, PATH

In MORSE-SGC/S, path-length stretching is accomplished by selecting the number of mean-free paths η to the next collision site from the probability density function (pdf)

$$\hat{f}(\eta) = [1 - \text{PATH}(IG,IR) * DIREC] \times \exp \{ - [1 - \text{PATH}(IG,IR) * DIREC]\eta \} , \tag{6}$$

where *DIREC* is the cosine of the angle between the particle direction and a vector specifying the most important direction of particle transport. Both *DIREC* and PATH(*IG,IR*) are input parameters each with values between -1 and 1. For positive values of PATH, particle path lengths are stretched toward the most important direction; for negative values of PATH, path lengths are shrunk toward this direction. If either PATH or *DIREC* equals 0, no path-length biasing takes place, and η is sampled from the natural pdf, $\exp(-\eta)$.

In this work, PATH(*IG,IR*) is determined by considering only those particles traveling in the most important direction (i.e., *DIREC* = 1). Then, PATH(*IG,IR*) is used in Eq. (6) for selection of η for all particles. For spent fuel cask problems, the most important directions are the outward radial vector for radial detectors and axially toward the top or bottom surfaces for axial detectors. For particles traveling in the most important direction, the path length is selected from the pdf,

$$\hat{f}_1(\eta) = [1 - \text{PATH}(IG,IR)] \times \exp \{ - [1 - \text{PATH}(IG,IR)]\eta \} . \tag{7}$$

A good approximation to the optimal pdf (Ref. 7) is

$$\hat{f}_2(\eta) = \frac{W(IG,IM)\exp(-\eta)}{\int W(IG,IM)\exp(-\eta)d\eta} , \tag{8}$$

where *W(IG,IM)* is the event-value function from the adjoint discrete-ordinates XSDRNPM-S calculation for a particle at spatial interval *IM* and energy group *IG* traveling in the most forward direction.

To illustrate the procedure for determination of PATH, let $W \sim \exp(c\eta)$, where $c < 1$. Then, from Eq. (8),

$$\hat{f}_2(\eta) = (1 - c)\exp[-(1 - c)\eta] \ . \tag{9}$$

Comparison of Eq. (9) with Eq. (7) shows that PATH = c. Of course, the event-value function will not have this simple exponential form. However, determination of PATH in such a manner that the error between exp(PATH * η) and W is minimized should result in appropriate values of PATH. This determination is done using the least-squares procedure outlined below.

Initially, consider the determination of $PATH_k$, where k is a spatial interval index in the XSDRNPM-S calculation as shown in Fig. 1. (The energy dependency is implied.) Let $\eta_{k,i}$ be the number of mean-free paths between intervals k and i. The following data points are available to estimate appropriate values of PATH: $[\eta_{k,i}; W(i)]$ for $i = k$ to IMAX.

We want to fit these data to

$$W(i) = W(k)\exp(PATH_k * \eta_{k,i}) \quad \text{for } i = k \text{ to IMAX} \tag{10}$$

or

$$PATH_k * \eta_{k,i} = \ln[W(i)/W(k)] \ .$$

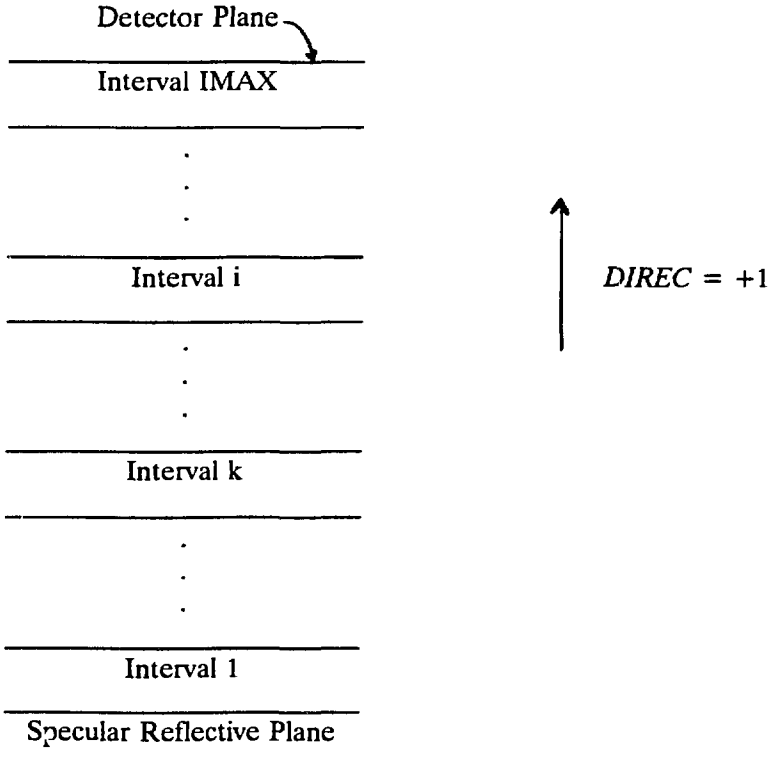

Fig. 1. The XSDRNPM-S interval notation used to obtain path-length stretching parameters, PATH.

The sum of the square errors will be

$$\epsilon_k^2 = \sum_{i=k}^{IMAX} [\ln W(i) - \ln W(k) - \mathrm{PATH}_k * \eta_{k,i}]^2 . \qquad (11)$$

Setting the derivative of ϵ_k^2 with respect to PATH_k to 0 leads to the following expression:

$$\mathrm{PATH}_k = \frac{\sum_{i=k}^{IMAX} \eta_{k,i}[\ln W(i) - \ln W(k)]}{\sum_{i=k}^{IMAX} \eta_{k,i}^2} . \qquad (12)$$

The values of PATH_k are calculated for each interval in a given region, and an average is taken to obtain the region-dependent PATH parameters. This procedure is done for all energy groups.

III.D FISSION NEUTRON WEIGHTS, FWLO

In MORSE-SGC/S, the population of fission neutrons can be regulated by the statistical weights given to fission neutrons at their birth. To have an efficient Monte Carlo calculation, the region- and energy-dependent fission neutron weights should be consistent with the biasing schemes used in a calculation. The Russian roulette survival weights, WTAV(*IG,IR*) of Eq. (2) are the appropriate values to use. However, the current version of MORSE-SGC/S does not allow input of these parameters as a function of energy group. Therefore, a group-averaged value of WTAV is needed. If the simple average is used for a given region, FWLO will be primarily determined by the WTAV value corresponding to low-importance particles because energy groups with low ϕ^* have high WTAV values [see Eq. (2)]. To avoid this problem, we weight WTAV with the fission spectrum of the spent fuel, FSE(*IG*,1); i.e.,

$$\mathrm{FWLO}(IR) = \sum_{IG} \mathrm{WTAV}(IG,IR) * \mathrm{FSE}(IG,1) . \qquad (13)$$

Although the fission spectrum corresponding to the medium in region *IR* would be more appropriate, the fission spectrum in the spent fuel region is usually similar enough to that of region *IR* that this approximation has no significant effect on the calculation. This approximation enables one to calculate FWLO without first determining the fission medium in region *IR* and avoids the problem that would be encountered if more than one fissionable medium were present in region *IR*.

III.E NEXT-EVENT ESTIMATION PROBABILITIES, PROB

The idea of the next-event estimation probabilities is not new and has been an option in major Monte Carlo transport codes such as TRIPOLI[10] and MCNP[11] for some time. Normally, when one uses a next-event estimator to point detectors or other types of detectors, an estimate to each detector position is made at all collision sites. The computational time required for this estimation process often exceeds the time required to generate and process the particle histories. This estimation from all collision sites can be very wasteful. For example, in the source region where a large number of collisions occur, the next-event contribution of the particle to detectors outside a

cask is often insignificant. This inefficiency can be reduced without biasing the effect of interest, λ, by estimating from a given region, *IR*, with a probability PROB(*IR*) and, if the estimation is made, dividing the contribution by PROB(*IR*); i.e.,

$$\begin{aligned}\lambda &= \sum_{IR} N(IR)\xi(IR) \\ &= \sum_{IR} [N(IR) * \mathrm{PROB}(IR)]\left(\frac{\xi(IR)}{\mathrm{PROB}(IR)}\right) \\ &= \sum_{IR} M(IR)\hat{\xi}(IR) \ , \end{aligned} \tag{14}$$

where

$N(IR)$ = collisions per history in region *IR*

$\xi(IR)$ = average, next-flight contributions of a particle having a collision in *IR* in standard game

$M(IR)$ = $N(IR)$ * PROB(*IR*) = number of estimates from region *IR* in the modified game

$\hat{\xi}(IR)$ = $\xi(IR)$/PROB(*IR*) = contribution in the modified game.

Although estimation probabilities are not normally used in MORSE-SGC/S, their implementation is simple and their effectiveness is apparent. Reasonable values for PROB can be determined from mean-free-path, WTAV, and response function considerations—all quantities can be calculated before the Monte Carlo calculation.

In this work, we set PROB(*IR*) such that the average next-event contribution from each region, *IR*, to the detector is the same. By requiring the contribution to be uniform throughout the system, the variance of λ should be reduced. The next-event contribution from a region can be approximated as

$$\lambda_{IR} \sim \sum_{IG} \mathrm{WTAV}(IG,IR) * R(IG) * \exp[-\eta(IG,IR)] \ , \tag{15}$$

where

$R(IG)$ = response function

$\eta(IG,IR)$ = number of mean-free paths between the midpoint of region *IR* and the detector in the XSDRNPM-S geometry (see Fig. 1).

PROB(*IR*) is then obtained with the following equation:

$$\mathrm{PROB}(IR) = \frac{\lambda_{IR}}{\lambda_{max}} \ , \tag{16}$$

where λ_{max} is the largest λ_{IR}.

In principle, PROB(*IR*) should increase monotomically with the region number, *IR*, and should be unity for the last region. However, it was found that Eqs. (15) and (16) do not lead to a maximum PROB for the last region for gamma-ray problems. This results in very inefficient calculations. Further examination revealed that WTAV(*IG,IR*) has extremely high values for low-energy gamma rays in the inner regions. The high WTAV values are due to the low ϕ^* of the inner regions [see Eq. (2)]. To overcome this problem, WTAV has been deleted from Eq. (15). The next-event contribution from region *IR* is then reduced to

$$\lambda_{IR} \sim \sum_{IG} R(IG) * \exp[-\eta(IG,IR)], \qquad (17)$$

and PROB*(IR)* is calculated from Eqs. (17) and (16) instead.

Since this procedure is a fair game, any values of PROB between 0 and 1 will, as the number of histories goes to infinity, produce the correct answer. However, from a practical standpoint, if PROB*(IR)* is very small, few or no estimates will be made from region *IR* and could lead to erratic results. Therefore, to allow for the approximate nature of λ_{IR}, PROB*(IR)* is required to be >0.001.

Finally, for situations where azimuthal symmetry exists, point detector are replaced by ring detectors to improve the efficiency of the calculation. This technique is described in detail in Refs. 12 and 13.

IV. APPLICATIONS AND RESULTS

The automated biasing procedure for an adjoint calculation, biasing parameters generation, and a Monte Carlo calculation of dose rates outside a spent fuel cask has been implemented in the SAS4 module[1] of the SCALE system. A depleted uranium cask had been analyzed and good agreement with 2-D discrete ordinates was obtained.[14] In this paper, analyses of a series of cast-iron casks of varying complexities were performed using the automated procedure. These casks include a simple geometry cask as defined by the NEACRP[5] working group and a transport cask[6] loaded with 12 PWR spent fuel assemblies. For comparison and verification, multiple solutions were obtained for a variety of computational methods including point and multigroup Monte Carlo, discrete-ordinates, and point-kernel methods.

IV.A NEACRP CAST-IRON CASK ANALYSIS

The first cask analyzed has been used as one of the problems for the international intercomparison of codes for transport cask shielding calculations sponsored by the Committee on Reactor Physics of the Nuclear Energy Agency. The geometry of this cask is quite simple and is shown in Fig. 2. The cask is composed of a source region and a cask body. The source region has a radius of 40 cm and a height of 450 cm and is entirely filled with a homogeneous spent fuel material.

The cask body is composed of cast iron, with both the wall and the base having thicknesses of 38 cm. The lid is stainless steel of 42-cm thickness. A modified version of the SCALE 27n-18g cross-section library is used for this problem. The dose response functions used were based on the ANSI/ANS 6.1.1 (1977) standard.[15] The sources are isotropic and uniformly distributed over the entire source region.

Neutron and primary gamma-ray responses were evaluated for radial and axial detector locations. For each response function (neutron or gamma-ray response function), radial and axial doses required separate sets of adjoint XSDRNPM-S and MORSE-SGC/S calculations to carry out the automated biasing procedure. In each Monte Carlo calculation, there are four surface detectors and three point detectors. The point detectors are 1, 2, and 10 m, respectively, from the outer

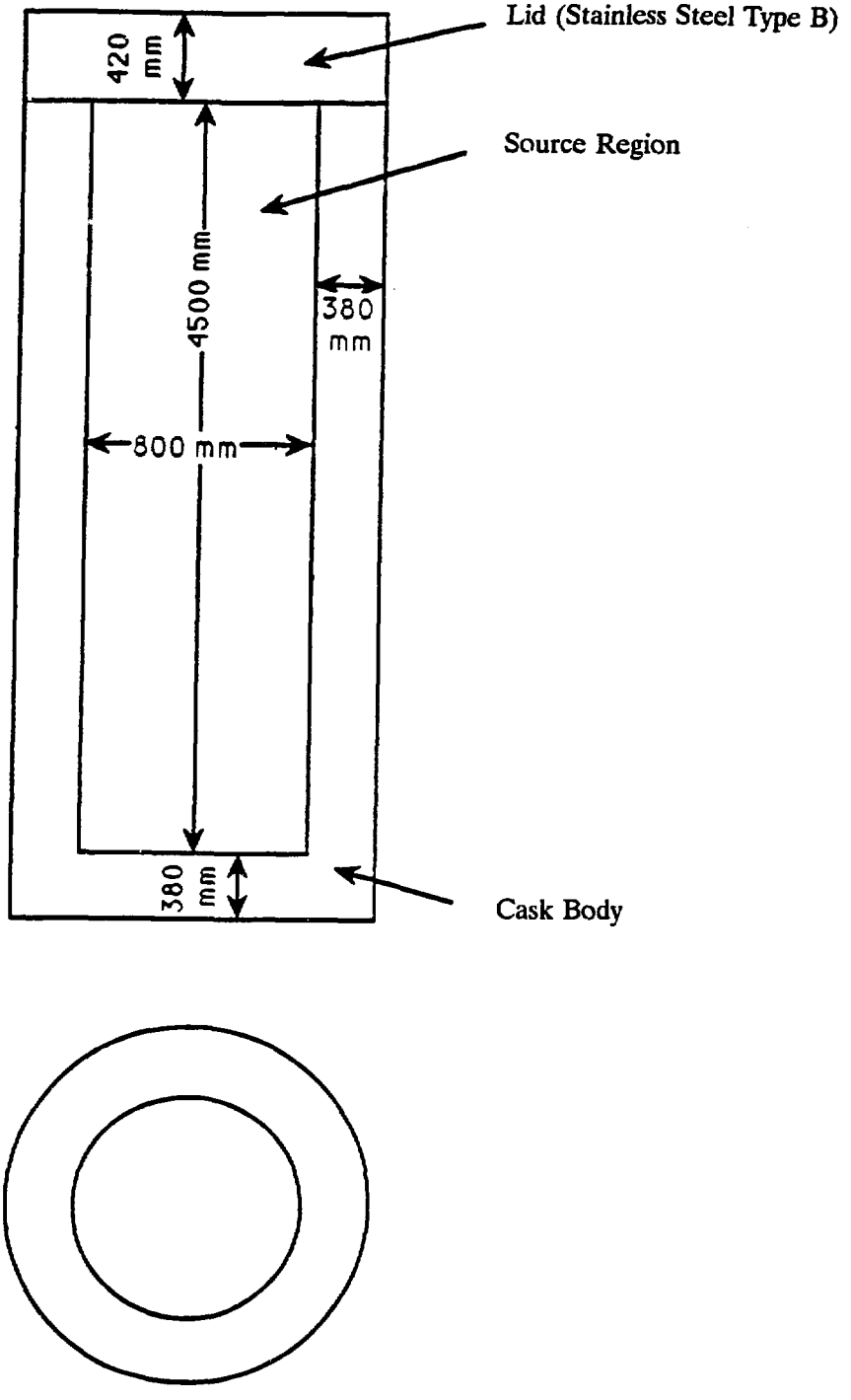

Fig. 2. Geometry of the NEACRP cast-iron cask.

radial or axial surface. The surface detectors are on the cask outer surface and are 1, 2, and 3 m, respectively, from this surface.

Results of calculations for this cask are presented in Table 1. These results are presented only at the cask surface. The results for locations away from the cask surface are given in Ref. 16.

In Table 1, the number of histories processed were 200 per batch for 50 batches for the neutron cases, 3000 per batch for 70 batches for the FP gamma cases, and 150 per batch for 80 batches for the capture gamma cases. The typical running time for a neutron case was 30 min., and less than 60 min. for a gamma-ray case on a CRAY computer.

The sidewall surface doses given in Table 1 show excellent agreement between the 1-D SAS1[2] values and the 2-D DORT[17] values. An interesting effect can be observed by comparing these 1-D values (using a 0.5-cm mesh in the shield) with the 2-D values (using a 1.0-cm mesh in the shield). The two neutron cases with a homogeneous shield (1a and 1c) give essentially identical results, while the two-material shield (1b) results are about 15% different. A similar effect is also seen for the fission-product gamma results. When the DORT mesh is refined to 0.5 cm, each of these cases then agrees well with the fine mesh 1-D results. Thus, for fission-product gammas transport through heterogeneous shields the mesh needs to be finer for a given degree of accuracy.

The QAD-CGGP[18] results shown in Table 1 indicate that for this problem the point-kernel technique performs quite well. The QAD-CGGP results are, in general, 15–20% high compared to the discrete-ordinates values. In this instance, the QAD-CGGP result that compares best with the discrete-ordinates results is that for the multiregion shield. This result is most likely fortuitous since the approximations within QAD-CGGP are less accurate for multiregion shields. Previous work[16] has shown that while QAD-CGGP performs well on the cask surface, it tends to be overly conservative 10 m away from the surface.

The DORT, SAS4, and MCNP results for the sidewall surface-averaged doses allow for several different comparisons to be made. First, the results labeled DORT-avg give the 2-D discrete-ordinates solution averaged over the cavity height. The SAS4-avg results utilize the same multigroup cross sections as the DORT-avg case but employ the Monte Carlo method. Both methods give results that agree to 10% or better. The MCNP fission-product (FP) gamma results similarly agree to within 10%. For the neutrons, the agreement is only about 20%, with the point cross sections giving higher results than the multigroup cross sections. The most likely cause is the better representation of the iron neutron cross-section minima with the point cross-section data. Lack of an appropriate multigroup cross-section library for this problem thus appears to induce a 20% error in the neutron dose with the multigroup codes.

The results for the cask lid and bottom surface doses follow somewhat similar trends as those of the surface sidewall. The FP gamma results are all very consistent as was seen before. The agreement between the multigroup discrete-ordinates and Monte Carlo results continues to be good. The comparison between the continuous energy (MCNP) and multigroup neutron results is somewhat confusing in that the 20% trend seen at the sidewall surface is not maintained. In fact, the agreement at the bottom is much better (2% between the DORT and MCNP) and much worse at the top (60% difference between DORT and MCNP).

IV.B TN-12 CASK ANALYSIS

To further demonstrate the applicability of the automated biasing procedure, the TN-12 transport cask was analyzed and comparisons made to a series of measured dose rates. This problem was also analyzed by the NEACRP working group on transport cask shielding. A detailed description of the TN-12 cask is given in NEACRP-A-961.[6] The cask was loaded with 12 PWR

Table 1. Summary results of NEACRP problem 1[a]

Surface doses (μSv/h)

	Neutron			FP gamma			Capture gamma		
	a	b	c	a	b	c	a	b	c
Sidewall									
QAD	–	–	–	296	1336	203	–	–	–
SAS1	517	53.7	47.1	268	1300	185	4.1	40.6	0.30
DORT	518	45.8[d]	47.2	240[d]	1168[d]	166[d]	4.1	49.9	0.30
DORT-avg[b]	485	40.1	45.8	233	1134	162	3.81	45.8	0.29
SAS4-avg	476(4)[c]	51.3(2)	48.0(4)	260(3)	1244(5)	193(3)	3.53(4)	38.5(3)	0.30(5)
MCNP-avg	589(2)	–	–	279(6)	–	–	–	–	–
Lid									
QAD	–	–	–	35.6	35.6	22.8	–	–	–
DORT	413	412	47.0	36.7	36.7	25.8	2.8	2.8	0.26
DORT-avg	313	312	36.1	31.4	23.1	16.4	2.19	2.18	0.20
SAS4-avg	304(6)	284(5)	37.0(10)	26.6(7)	24.5(8)	17.7(7)	2.31(16)	2.45(11)	0.19(13)
MCNP-avg	524(6)	–	–	29.0(8)	–	–	–	–	–
Bottom									
QAD	–	–	–	382	382	245	–	–	–
DORT	541	541	61.5	403	403	287	3.9	3.9	0.38
DORT-avg	410	410	47.4	291	267	190	3.11	3.08	0.30
SAS4-avg	352(7)	385(10)	41.3(8)	325(10)	252(7)	183(9)	2.78(8)	2.74(13)	0.28(16)
MCNP-avg	422(7)	–	–	316(10)	–	–	–	–	–

[a]Case a = dry fuel, 38-cm solid cast iron shield.
Case b = dry fuel, 32-cm cast iron with 6 cm polyethylene.
Case c = wet fuel, 38-cm solid cast iron shield.
Calculations with SAS1, DORT, and SAS4 performed using 27n-18g group cross sections (ENDF/B-V).
QAD used built-in attenuation data and log-log interpolation.

[b]"avg" indicates dose is averaged over cavity height for the sidewall doses and over cavity diameter for axial doses. Otherwise, point detectors are used and located at the axial midplane for the sidewall doses and at the radial center for the axial doses.

[c]Number in parentheses indicates percent standard deviation.

[d]Upon rerunning with a finer spatial mesh, agreement with the SAS1 results is obtained.

spent fuel assemblies from Unit 1 of the Fessenheim Nuclear Power Plant. Some assemblies had been irradiated for only one cycle, while others were irradiated for two cycles. The TN-12 cask consists of a cylindrical cavity of diameter 122-cm housing 12 PWR fuel assemblies as shown in Fig. 3. The cask body consists of a 30-cm-thick forged carbon-steel shield clad with stainless steel to provide for attenuation of gamma radiation. The neutron shield is made from resin 10-cm thick surrounding the cask body and traversed by nickel-copper cooling fins. The 3-D model represented the fuel assemblies in a smeared fashion while explicitly modeling the cavity basket and gamma shield. The neutron shield and corresponding fin portions penetrating the neutron shield were smeared such that the explicit geometry was not modeled. All results presented in the following tables are for smeared fins. Estimates performed separately by applying an approximate fin model determined effects of only 3-5% for a smeared vs explicit fin model. Thus, no correction was applied to account for the discrete vs smeared fin models.

The results shown in Tables 2 and 3 give comparisons between the SAS4 predictions and measurements for the neutron and gamma-ray dose rates, respectively. These comparisons are given near the cask surface and in some cases 1 and 2 m from the cask surface for three locations, the axiai mid-height, the top peak and the bottom peak along the cask side. The neutron results in Table 2 were calculated from processing 140 batches of 200 histories per batch, and the CPU time was about one hour. The gamma-ray results in Table 3 were obtained from 1200 batches of 2000 histories per batch, and the CPU time was about 5 hr. The neutron predictions are somewhat higher than the measured values; however, problems were found in the neutron measurements that could easily account for these differences. The neutron detector responses were initially believed to represent the neutron dose rate. This was later found to be untrue. The calculations given in Table 2 utilized an approximate detector response function that was subsequently issued informally to the working group.

The gamma-ray results produced by SAS4 and an alternate solution by the QAD-CGGP code are given in Tables 3 and 4, respectively. Both sets of calculated results yield acceptable agreement with the measurements. The QAD-CGGP results are uniformly within 20% of the measured values, while, in general, the SAS4 results also fall within this range. Due to the statistical nature of Monte Carlo and, in particular, the point detectors as utilized here, several of the SAS4 results fall outside the 20% range but still lie within 2σ of the Monte Carlo statistics. The two exceptions to this trend occur at the bottom of the cask where the 0.65 and 0.64 C/E's differ by some 5-6σ's.

These results suffer from the classical pitfall of undersampling of point-detector response whereby the majority of the contribution comes from particles very far away (greater than 10 mean-free paths) from the point detectors. The combination of low responses (C/E of 0.65 and 0.64) and low uncertainties (6% standard deviations) strongly support this observation. In fact, if we examine the top and bottom responses in Table 3, six of seven responses with C/E less than 1.0 have a standard deviation less than 7%. However, all results with C/E greater than one have a standard deviation greater than 14%. The results at the top and bottom locations are the consequences of undersampling due to the source axial burnup profile which started very few particles near the ends of the cask.

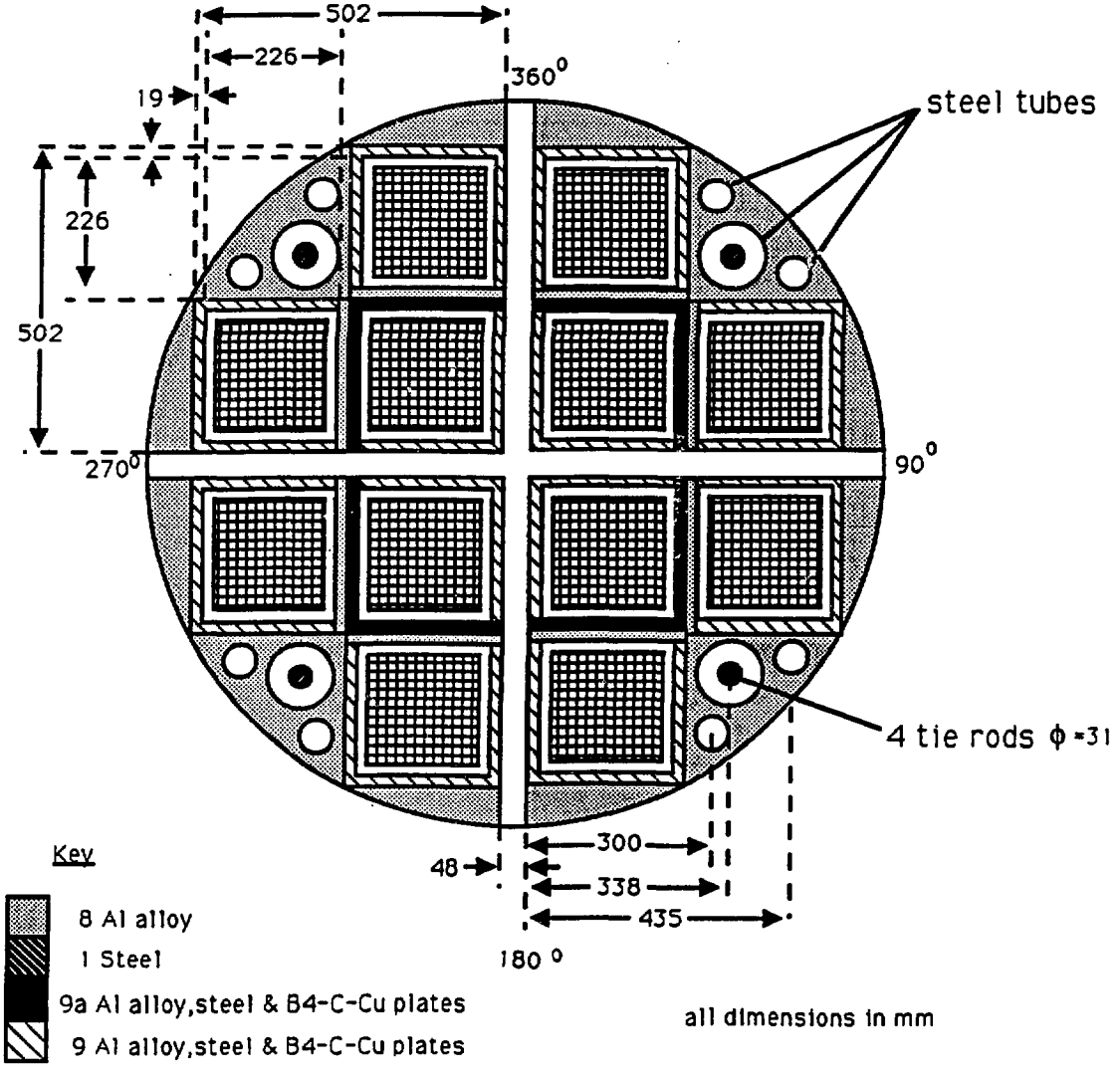

Fig. 3. Cross-sectional view of the TN-12 cask.

Table 2. TN-12 Neutron dose rates at $\theta = 90°$ (SAS4)

Dose point	Distance from fin tips (cm)	Experiment		Calculation	
		Dose rate (μ Sv/h)	Z[a] (cm)	Dose rate (μ Sv/h)	C/E
Peak at bottom of flask	15.5	35.0	47.5	48.6 ± 60%	1.39
Peak of top of flask	15.5	59.3	467.0	62.2 ± 17%	1.05
At mid-height of active fuel	15.5	52.9	271.9	79.3 ± 7%	1.50
	100	28.6	271.9	36.9 ± 4%	1.29
	181.5	19.0	271.9	21.6 ± 3%	1.14

[a]Z = height above bottom of flask.

Table 3. TN-12 gamma-ray dose rates (SAS4)

			Experiment		Calculation	
Dose point	θ	Distance from fin tips (cm)	Dose rate (μ Sv/h)	Z (cm)	Dose rate (μ Sv/h)	C/E
Peak at bottcm of flask	135°	7	150	118.0	97.5 ± 6%	0.65
	153°	7	162	118.0	176.2 ± 36%	1.09
		100	54	108.0	50.2 ± 18%	0.93
	180°	7	145	112.0	92.4 ± 6%	0.64
Peak of top of flask	135°	7	210	420.0	274.1 ± 20%	1.31
		200	39	402.0	48.1 ± 22%	1.23
	153°	7	248	416.0	237.9 ± 7%	0.96
		100	80	402.0	72.2 ± 5%	0.90
		200	42	405.0	37.7 ± 5%	0.90
	180°	7	210	417.0	221.6 ± 14%	1.06
		200	38	396.0	35.8 ± 6%	0.94
At mid-height of active fuel	135°	7	80	271.9	92.6 ± 9%	1.16
		200	31	271.9	32.4 ± 3%	1.05
	153°	7	97	271.9	102.1 ± 5%	1.05
		100	49	271.9	58.4 ± 11%	1.19
		200	33	271.9	38.0 ± 10%	1.15
	180°	7	79	271.9	108.1 ± 20%	1.37
		200	31	271.9	34.1 ± 4%	1.10

Table 4. TN-12 gamma-ray dose rates (QADS)

			Experiment		Calculation	
Dose point	θ	Distance from fin tips (cm)	Dose rate (μ Sv/h)	Z (cm)	Dose rate (μ Sv/h)	C/E
Peak at bottom of flask	135°	7	150	118.0	136	0.91
	153°	7	162	118.0	172	1.06
		100	54	108.0	63	1.17
	180°	7	145	112.0	140	0.93
Peak of top of flask	135°	7	210	420.0	190	0.90
		200	39	402.0	41	1.05
	153°	7	248	416.0	219	0.88
		100	80	402.0	86	1.08
		200	42	405.0	43	1.02
	180°	7	210	417.0	186	0.89
		200	38	396.0	39	1.03
At mid-height of active fuel	135°	7	80	271.9	87	1.09
		200	31	271.9	37	1.19
	153°	7	97	271.9	104	1.07
		100	49	271.9	58	1.18
		200	33	271.9	39	1.18
	180°	7	79	271.9	84	1.06
		200	31	271.9	36	1.16

V. CONCLUSIONS

The results obtained for neutron and gamma-ray responses of numerous spent fuel casks indicate that with the automated biasing procedure, Monte Carlo shielding analyses of spent fuel casks can be performed with minimum effort and that accurate and reliable results can be obtained. The major task of setting up biasing parameters in a Monte Carlo deep-penetration calculation has been eliminated. With the automated procedure, the difficulty of carrying out a 3-D analysis of spent fuel casks has been greatly reduced.

However, further study is still needed to improve calculation of the corner doses. One possible solution is to allow source axial biasing in the radial calculation so that more source particles start from the ends of the cask. Another approach may be to develop 2-D importance functions for the corner detectors. Finally, the systematic biasing approach described in this paper can be applied to other Monte Carlo shielding problems.

VI. REFERENCES

1. J. S. TANG, "SAS4: A Monte Carlo Cask Shielding Analysis Module with Automated Biasing Procedure," see Sect. S4 of *SCALE: A Modular Code System for Performing Standardized Computer Analyses for Licensing Evaluation*, NUREG/CR-0200, Rev. 4 (ORNL/NUREG/CSD-2/R4), Vols. I, II, and III (draft February 1990). Available from Radiation Shielding Information Center at Oak Ridge National Laboratory as CCC-545.

2. *SCALE: A Modular Code System for Performing Standardized Computer Analyses for Licensing Evaluation*, NUREG/CR-0200, Rev. 4 (ORNL/NUREG/CSD-2/R4), Vols. I, II, and III (draft February 1990). Available from Radiation Shielding Information Center at Oak Ridge National Laboratory as CCC-545.

3. G. GOERTZEL and M. H. KALOS, *Progress in Nuclear Energy*, Vol. 2, p. 315, Pergamon Press, Inc., New York (1958).

4. J. E. HOOGENBOOM, *Nucl. Sci. Eng.* **70**, 210 (1979).

5. A. F. AVERY and H. F. LOCKE, *NEACRP Intercomparison of Codes for the Radiation Protection Assessment of Transportation Packages. Solutions to Problems 1-4*, NEACRP-L-331 (March 1992).

6. C. M. DIOP, J. C. NIMAL, P. BLUM, and R. CAGNON, *TN12 Shipping Cask Calculations Benchmark*, NEACRP-A-961 (January 1989).

7. J. S. TANG, T. J. HOFFMAN, and P. N. STEVENS, *Nucl. Sci. Eng.* **62**, 617 (1977).

8. J. S. TANG, T. J. HOFFMAN, and P. N. STEVENS, *Nucl. Sci. Eng.* **64**, 837 (1977).

9. R. R. COVEYOU, V. R. CAIN, and K. J. YOST, *Nucl. Sci. Eng.* 27, 219 (1967).

10. J. C. NIMAL et al., *Programme de Monte Carlo polycinetique á trois dimensions TRIPOLI*, CEA.N.1919, Commissariat á l'Energie Atomique, Saclay (1976).

11. *MCNP - A Generalized Monte Carlo Code for Neutron and Photon Transport*, LA-7396-M, Los Alamos National Laboratory (1981).

12. J. E. STEWART, *Trans. Am. Nucl. Soc.* **28**, 643 (1978).

13. T. J. HOFFMAN and J. S. TANG, *XSDRNPM-S Biasing of MORSE-SGC/S Shipping Cask Calculations*, ORNL/CSD/TM-175, Union Carbide Corp., Nucl. Div., Oak Ridge Natl. Lab. (1982).

14. J. S. TANG and T. J. HOFFMAN, *Nucl. Sci. Eng.* **99**, 329 (1988).

15. *ANSI/ANS-6.1.1-1977, Neutron and Gamma-Ray Flux-to-Dose-Rate Factors*, American Nuclear Society, LaGrange Park, Illinois (1977).

16. B. L. BROADHEAD, M. C. BRADY, and C. V. PARKS, *Benchmark Shielding Calculations for the NEACRP Working Group on Shielding Assessment of Transportation Packages*, ORNL/CSD/TM-272, Martin Marietta Energy Systems, Inc., Oak Ridge Natl. Lab. (November 1990).

17. W. A. RHOADES and R. L. CHILDS, *Two- and Three-Dimensional Discrete Ordinates Transport*, January 1992. Available from Radiation Shielding Information Center at Oak Ridge National Laboratory as CCC-543/TORT-DORT.

18. *QAD-CGGP. A Combinatorial Geometry Version of QAD-P5A. A Point Kernel Code System for Neutron and Gamma-Ray Shielding Calculations Using the GP Build-up Factor.* Available from Radiation Shielding Information Center at Oak Ridge National Laboratory as CCC/493/QAD-CGGP.